Behavioral/Cognitive

Enhancement of Haloperidol-Induced Catalepsy by GPR143, an L-Dopa Receptor, in Striatal Cholinergic Interneurons

Masami Arai,[1] Etsuko Suzuki,[2] Satoshi Kitamura,[1] Momoyo Otaki,[1] Kaori Kanai,[1] Miwako Yamasaki,[3] Masahiko Watanabe,[3] Yuki Kambe,[4] Koshi Murata,[5] Yuuki Takada,[6] Tetsu Arisawa,[6,7] Kenta Kobayashi,[8] Rei Tajika,[1] Tomoyuki Miyazaki,[6] Masahiro Yamaguchi,[9] Michael Lazarus,[10,11] Yu Hayashi,[11,12] Shigeyoshi Itohara,[13] Alban de Kerchove d'Exaerde,[14] Hiroyuki Nawa,[15] Ryang Kim,[16] Haruhiko Bito,[16] Toshihiko Momiyama,[2] Daiki Masukawa,[1] and Yoshio Goshima[1]

[1]Department of Molecular Pharmacology and Neurobiology, Yokohama City University Graduate School of Medicine, Yokohama 236-0004, Japan, [2]Department of Pharmacology, Jikei University School of Medicine, Tokyo 105-8461, Japan, [3]Department of Anatomy, Faculty of Medicine, Hokkaido University, Sapporo 060-8638, Japan, [4]Department of Pharmacology, Graduate School of Medical and Dental Science, Kagoshima University, Kagoshima 890-0075, Japan, [5]Division of Brain Structure and Function, Faculty of Medical Sciences, University of Fukui, Fukui 910-0017, Japan, [6]Department of Physiology, Yokohama City University Graduate School of Medicine, Yokohama 236-0004, Japan, [7]Radioisotope Research Center, Yokohama City University Graduate School of Medicine, Yokohama 236-0004, Japan, [8]Section of Viral Vector Development, Center for Genetic Analysis of Behavior, National Institute for Physiological Sciences, Okazaki 444-8585, Japan, [9]Department of Physiology, Kochi Medical School, Kochi University, Kochi 783-8505, Japan, [10]Institute of Medicine, University of Tsukuba, Tsukuba 305-0005, Japan, [11]International Institute for Integrative Sleep Medicine (WPI-IIIS), University of Tsukuba, Tsukuba 305-0005, Japan, [12]Department of Biological Sciences, Graduate School of Science, University of Tokyo, Tokyo 113-0033, Japan, [13]Laboratory for Behavioral Genetics, RIKEN Center for Brain Science, Wako, Saitama 351-0198, Japan, [14]Neurophy Lab, ULB Neuroscience Institute, Université Libre de Bruxelles (ULB), Brussels B-1070, Belgium, [15]Department of Physiological Sciences, School of Pharmaceutical Sciences, Wakayama Medical University. Wakayama-city, Wakayama 640-8156, Japan, and [16]Department of Neurochemistry, Graduate School of Medicine, The University of Tokyo, Tokyo 113-0033, Japan

Dopamine neurons play crucial roles in pleasure, reward, memory, learning, and fine motor skills and their dysfunction is associated with various neuropsychiatric diseases. Dopamine receptors are the main target of treatment for neurologic and psychiatric disorders. Antipsychotics that antagonize the dopamine D2 receptor (DRD2) are used to alleviate the symptoms of these disorders but may also sometimes cause disabling side effects such as parkinsonism (catalepsy in rodents). Here we show that GPR143, a G-protein-coupled receptor for L-3,4-dihydroxyphenylalanine (L-DOPA), expressed in striatal cholinergic interneurons enhances the DRD2-mediated side effects of haloperidol, an antipsychotic agent. Haloperidol-induced catalepsy was attenuated in male *Gpr143 gene*-deficient (*Gpr143*$^{-/y}$) mice compared with wild-type (Wt) mice. Reducing the endogenous release of L-DOPA and preventing interactions between GPR143 and DRD2 suppressed the haloperidol-induced catalepsy in Wt mice but not *Gpr143*$^{-/y}$ mice. The phenotypic defect in *Gpr143*$^{-/y}$ mice was mimicked in cholinergic interneuron-specific *Gpr143*$^{-/y}$ (*Chat-cre;Gpr143*$^{flox/y}$) mice. Administration of haloperidol increased the phosphorylation of ribosomal protein S6 at Ser$^{240/244}$ in the dorsolateral striatum of Wt mice but not *Chat-cre;Gpr143*$^{flox/y}$ mice. In Chinese hamster ovary cells stably expressing DRD2, co-expression of GPR143 increased cell surface expression level of DRD2, and L-DOPA application further enhanced the DRD2 surface expression. Shorter pauses in cholinergic interneuron firing activity were observed after intrastriatal stimulation in striatal slice preparations from *Chat-cre;Gpr143*$^{flox/y}$ mice compared with those from Wt mice. Together, these findings provide evidence that GPR143 regulates DRD2 function in cholinergic interneurons and may be involved in parkinsonism induced by antipsychotic drugs.

Key words: **antipsychotic; dopamine D2 receptor; GPR143; L-DOPA; parkinsonism; striatum**

Received July 31, 2023; revised Nov. 30, 2023; accepted Jan. 11, 2024.

Author contributions: M.A., E.S., S.K., M.O., K.K., M.Y., M.W., Y.K., K.M., Y.T., T.A., K.K., R.T., T.M., M.Y., M.L., Y.H., S.I., A.K.D., H.N., H.B., T.M., D.M., and Y.G. designed research; M.A., E.S., S.K., M.O., K.K., M.Y., M.W., Y.K., K.M., Y.T., T.A., K.K., R.T., T.M., M.Y., M.L., Y.H., S.I., A.K.D., H.N., R.K., H.B., T.M., D.M., and Y.G. performed research; M.A., E.S., S.K., M.O., K.K., M.Y., M.W., Y.K., K.M., Y.T., T.A., K.K., R.T., T.M., M.Y., M.L., Y.H., S.I., A.K.D., H.N., R.K., H.B., T.M., D.M., and Y.G. analyzed data; M.A., E.S., S.K., M.O., K.K., M.Y., M.W., Y.K., K.M., Y.T., T.A., K.K., R.T., T.M., M.Y., M.L., Y.H., S.I., A.K.D., H.N., R.K., H.B., T.M., D.M., and Y.G. wrote the paper.

This work was supported by Scientific Research (B) (General) (18H02580 to Y.G.; 21H02673 to Y.G.); JP16H06276 (AdAMS) to Y.G.; Scientific Research (C) (General) (20K07069 to D.M.); Grant-in-Aid for Young Scientists (18K14923 to D.M.); and Foundation of Strategic Research Projects in Private Universities, from the Ministry of Education, Culture, Sport, Science, and Technology (MEXT) of Japan; the Japanese SRF Grant for Biomedical Research (2021G010 to D.M.); the JPMH KAKENHI (22KC1005). and the fund for Creation of Innovation Centers for Advanced Interdisciplinary Research Areas Program in the Project for Developing Innovation Systems from MEXT (42890001 to Y.G.); and Takeda Science Foundation (to D.M.), Uehara Memorial Foundation (201810115 to D.M.), and AMED (JP22ek0109431 to Y.G.). A.K.E. is supported by the Fund for Scientific Research (F.R.S-FNRS, Belgium). A.K.E. is a Research Director of the FNRS and a WELBIO Investigator. We thank K. Kobayashi (Fukushima Medical College) for valuable discussion and constructive input. We also thank T. Okada and Y. Nakamura for excellent technical assistance.

The authors declare no competing financial interests.

Correspondence should be addressed to Daiki Masukawa at masukawa@yokohama-cu.ac.jp or Yoshio Goshima at goshima@yokohama-cu.ac.jp.

https://doi.org/10.1523/JNEUROSCI.1504-23.2024

Significance Statement

Dopamine neuron systems play crucial roles in the control of multiple functions including cognition, fine motor skills and behavioral flexibility, and are involved in neurologic and psychiatric disorders. Antipsychotics are used to alleviate the positive symptoms of schizophrenia and other psychiatric disorders. The therapeutic efficacy of these drugs is related to their antagonistic activities against D2 receptors (DRD2), but disabling side effects may also be caused by DRD2 blockade in multiple dopaminergic pathways. L-DOPA receptor GPR143 when coupled with DRD2 potentiates DRD2-mediated signaling. The neuronal pathways is involved in the GPR143 function, however, have not yet been identified. Here, we identified cholinergic interneurons as the neural circuits in which DRD2 coupled with the L-DOPA receptor GPR143 mediates haloperidol-induced catalepsy.

Introduction

Dopamine (DA) neurons in the midbrain are involved in a wide variety of neurologic and psychiatric processes (Crittenden and Graybiel, 2011; Latif et al., 2021). Psychiatric disorders in which striatal dopaminergic neurons are excited highlight the importance of dopaminergic function (Wada et al., 2022). Although antipsychotics that antagonize DA D2 receptors (DRD2s) effectively alleviate some symptoms of psychiatric disorders, extrapyramidal symptoms (exhibited as catalepsy in rodents) are serious side effects of DRD2 antagonists, limiting their use and markedly affecting the patient's quality of life (Pani, 2002). Selective targeting of DRD2 populations may lead to the development of improved treatments for these devastating diseases.

Antipsychotics such as haloperidol are utilized to examine the role of DRD2-mediated dopaminergic transmission at the level of the neural circuit (Kharkwal et al., 2016; Waku et al., 2021). DRD2s are expressed in various neural circuits of the striatum, including indirect-pathway medium spiny neurons (iMSNs), dopaminergic and glutaminergic terminals, GABA interneurons, and cholinergic interneurons (Witten et al., 2010; Cachope et al., 2012; Nelson et al., 2014). DRD2s expressed in cholinergic interneurons represent only 1–2% of the striatal DRD2s. The importance of DRD2 function in the control of motor function (Tepper and Bolam, 2004) was recently elucidated by studies using mice with cell-type-specific DRD2 ablation in cholinergic interneurons (Kharkwal et al., 2016). DRD2 stimulation inhibits acetylcholine release (DeBoer et al., 1996). DA neuron firing induces a pause in striatal cholinergic interneuron firing activity and enhances DRD2-expressing iMSN activity by suppressing cortical inputs (Ding et al., 2010; Thorn and Graybiel, 2010; Tozzi et al., 2011; Threlfell et al., 2012). Haloperidol induces catalepsy in mice, and mice lacking DRD2s in cholinergic interneurons exhibit attenuated antipsychotic-induced parkinsonism (Kharkwal et al., 2016; Lewis et al., 2020).

L-3,4-Dihydroxyphenylalanine (L-DOPA), the most effective therapeutic agent for treating Parkinson disease (PD), is believed to act after its conversion to DA by aromatic L-amino acid decarboxylase (AADC) (Group et al., 2014). We have proposed that L-DOPA itself plays a role as a neurotransmitter (Misu et al., 1996; Goshima et al., 2019). Although the L-DOPA receptor has long been ill-defined, a G-protein coupled receptor (GPCR), GPR143, the gene product of ocular albinism 1 (Schiaffino et al., 1999), was shown to possess L-DOPA-binding activity and to mediate an intracellular Ca^{2+} response to L-DOPA in animal cells (Lopez et al., 2008), and to act as an L-DOPA receptor (Masukawa et al., 2017, 2023; Kasahara et al., 2022). Notably, L-DOPA induces functional coupling between GPR143 and DRD2. GPR143 interacts with DRD2 at the fifth transmembrane (TM5) domain and L-DOPA enhances this interaction (Masukawa et al., 2023). Enhancement of the interaction by L-DOPA is not observed in GPR143 knockout ($Gpr143^{-/y}$) mice. A peptide that interrupts the GPR143-DRD2 interaction mitigates the behavioral response to the DRD2 agonist quinpirole. The neural circuits involved in the GPR143-modulating effects of DRD2 function, however, are unknown.

Here we demonstrate that GPR143 regulates DRD2 function in striatal cholinergic interneurons. Haloperidol induced catalepsy in wild-type (Wt) mice, but the effect was attenuated in $Gpr143^{-/y}$ mice. The effects of haloperidol were suppressed by reducing the endogenous release of L-DOPA and preventing interactions between GPR143 and DRD2 in Wt mice but not in $Gpr143^{-/y}$ mice. The phenotypic defect in $Gpr143^{-/y}$ mice was mimicked in cholinergic interneuron-specific $Gpr143^{-/y}$ (*Chat-cre;*$Gpr143^{flox/y}$) mice. Re-expression of GPR143 in cholinergic interneurons of the dorsal striatum rescued the effect of haloperidol in $Gpr143^{-/y}$ mice. In the dorsolateral striatum of Wt mice, haloperidol increased the phosphorylation of ribosomal protein S6 (rpS6) at $Ser^{240/244}$ but this effect was not observed in *Chat-cre;*$Gpr143^{flox/y}$ mice. Cholinergic interneuron firing pauses after intrastriatal stimulation were shorter in *Chat-cre;* $Gpr143^{flox/y}$ mice than in control mice. Together, these findings indicate that GPR143 coupled with DRD2 enhances DRD2-mediated synaptic transmission in striatal cholinergic interneurons. Targeting GPR143 may help to reduce the extrapyramidal side effects of antipsychotics.

Materials and Methods

Ethics statement. All animal care and experimental procedures were conducted as recommended by the Guide for the Care and Use of Laboratory Animals in Yokohama City University Graduate School of Medicine (permission number: F-A-17-012 and F-A-20-017) and Jikei University School of Medicine (permission number: 2021-090 and D2021-082). Throughout the experimental procedures, all efforts were made to minimize the number of animals used and their suffering.

Animals. We previously generated $Gpr143^{-/y}$ and $Gpr143^{flox/y}$ mice in the C57BL/6J genetic background (Fukuda et al., 2015). Male $Gpr143^{-/y}$ and Wt mice from the same litter were used in the experiments. To determine whether nigrostriatal DA neurons release L-DOPA, we applied the DREADD (designer receptors exclusively activated by designer drugs) system to DA transporter (*Dat*)-cre mice. To investigate the role of neuron-specific GPR143, we generated mice lacking GPR143 in DRD2-, adenosine A2A receptor (ADORA2A)-, and choline acetyltransferase (ChAT)-positive neurons by crossing male $Gpr143^{flox/y}$ mice and female hemizygote *Drd2*-cre mice. Male *Adora2a*- and *Chat*-cre mice were mated with female $Gpr143^{flox/+}$ mice. The animal information is provided in Table 1. Mice (6–12 weeks old) weighing 20–25 g were used and housed in a temperature- (23 ± 1°C) and humidity- (55%) controlled room. The mice were maintained on a light-dark cycle (light

Table 1. Animals

Animals	Source (Reference)	ID Number	Provided by
Gpr143-/y	Fukuda et al. (2015)		
Gpr143flox	Fukuda et al. (2015)		
DRD2-cre	MMRRC	#032108-UCD	
ADORA2A-cre	MMRRC	#036158-UCD	
ChAT-cre	RIKEN BRC	#RBRC10635	Yu Hayashi
DAT-cre	Jackson	#020080	Xiaoxi Zhuang

Table 2. Viral vectors

Viral vector	Abbreviation	Serotype	Titer (vg/ml)	Injection volume
CAGGS-GPR143-2A-EGFP	GPR143	AAVdj	1.4×10^{12}	1 µl
CAGGS-EGFP	EGFP	AAVdj	8.0×10^{12}	0.5 µl
CAGGS-DIO-GPR143-2A-EGFP	DIO-GPR143	AAV9	2.0×10^{13}	1 µl
CAGGS-DIO-EGFP	DIO-EGFP	AAV9	2.0×10^{13}	1 µl
eSynI-DIO-hM3Dq-mCherry	DIO-hM3Dq-mCherry	AAV2/1	9.0×10^{12}	1 µl
CAGGS-DIO-mCherry	DIO-mCherry	AAV2/1	9.0×10^{12}	1 µl

period 07.00–19.00 h) with laboratory mouse food and water available ad libitum. Mice were habituated to handling by picking them up once a day for at least 3 d before the experiments were performed.

Drugs and TAT peptides. Haloperidol was purchased from Tokyo Kasei, DL-α-Methyltyrosine methyl ester (αMPT) was purchased from Nacalai Tesque, and clozapine-N-oxide (CNO) was purchased from Tocris. Transactivator of transcription transmembrane (TAT-TM) peptides were manufactured and purchased from GeneScript as previously described (Masukawa et al., 2023). The GPR143 peptide sequence was as follows: TAT-control, YGRKKRRQRRR; TAT-TM5, IPHYVTTYLPLLLVLVANPILYGRKKRRQRRR.

Assessment of catalepsy. Catalepsy was assessed using the bar test (Torigoe et al., 2012). The forelimbs of the mice were placed on a wire mesh stand 3 cm above a flat floor. The time until the mouse spontaneously removed its forelimbs from the wire, i.e., the duration of catalepsy, was measured every 30 min for 2 h after intraperitoneal (i.p.) administration of haloperidol (0.5 mg/kg). At 30 and 15 min before the administration of haloperidol, mice were administered α-methyl-p-tyrosine (αMPT, 3 mg/kg, i.p.) or TAT peptides [100 pmol, intracerebroventricular (i.c.v.) administration], respectively. The maximum duration of each measurement was 120 s. Measurements were averaged from the two measurements taken at each time point.

Surgery. To activate nigrostriatal DA neurons, we used *Dat-cre* mice. The mice were anesthetized with 2–3% isoflurane inhalation, and lidocaine (0.043 mg/kg) was administered to scalp subcutaneously, which induced a sufficient analgesic effect. After fixing the head of mice in a stereotaxic device, adeno-associated virus 2/1 (AAV2/1) encoding DIO-hM3Dq-mCherry and DIO-mCherry were microinjected into the substantia nigra (−3.0 mm anterior, 1.3 mm lateral, 4.3 mm deep from the bregma). Microdialysis was used to measure L-DOPA and DA released from the brain. The guide (AG-4) and dummy (AD-4) cannulas (Eicom, Kyoto, Japan) were inserted into the dorsolateral striatum (0.5 mm anterior, 2.2 mm left and right lateral, 2.8 mm deep from the bregma), and the microdialysis experiments were started 2 d after surgery.

For the rescue experiment, we used *Gpr143*$^{-/y}$ mice. AAVdj encoding mouse GPR143-P2A-enhanced green fluorescent protein (EGFP) or EGFP was stereotaxically injected into the dorsal striatum (0.5 mm anterior, 2.0 mm lateral, 3.5 mm deep from the bregma). For circuit-specific rescue analysis, *Drd2-cre;Gpr143*$^{-/y}$, and *ChAT-cre;Gpr143*$^{-/y}$ mice were injected with AAV9-DIO-GPR143-P2A-EGFP or AAV9-DIO-EGFP into the dorsal striatum. The AAV information is listed in Table 2. Two weeks after recovery, the behavioral analysis was performed. To confirm the expression of GPR143 and DRD2 in the GPR143-P2A-EGFP- or AAV9-DIO-GPR143-P2A-EGFP-injected group, we performed immunohistochemistry using anti-GPR143 and DRD2 antibodies (data not shown).

Measurement of L-DOPA and DA release. A microdialysis probe (FX-I-4-02, Eicom) was inserted into an implanted guide cannula, and Ringer's solution (147 mM Na^+, 2.3 mM Ca^{2+}, 4 mM K^+, and 155.6 mM Cl^-) was perfused at a flow rate of 2 µl/min. Dialysate was collected every 20 min before and after i.p. administration of αMPT (3 mg/kg), CNO (3 mg/kg), or saline. Samples were mixed with an equal volume of ultrapure water containing 0.1% formic acid and stored at −80°C until analysis. The levels of L-DOPA and DA were determined by liquid chromatography-mass spectrometry (LC-MS/MS; Xevo TQS, Waters). The analytical column was a UPLC column ACQUITY HSS T3 C18 (WT186003539, Waters) with a guard column (WT186003976, Waters). The mobile phase comprised ultrapure water containing 3% acetonitrile and 0.1% formic acid.

Immunohistochemistry and in situ hybridization. For double immunofluorescence, we used rabbit anti-tyrosine hydroxylase (TH) and guinea pig anti-AADC antibodies (listed in Table 3). Glyoxal-fixed (Konno et al., 2023) mouse coronal sections (20 µm in thickness) were incubated with 10% normal donkey serum for 20 min, and then a cocktail of primary antibodies diluted with phosphate-buffered saline (PBS) containing 0.1% Triton X-100 (PBS-T) overnight, followed by a mixture of with Cy3- and Alexa488-labeled species-specific secondary antibodies (1:200; Jackson ImmunoResearch) for 2 h. Images were obtained with a confocal laser-scanning microscopy (FV1200; Evident). The intensity of the immunofluorescence signals in the dorsal striatum and cerebral cortex was measured by setting microscopes at the same gain level. The signal intensity was measured using MetaMorph software (Molecular Devices). In brief, images were separated into individual channels, converted into grayscale, and thresholded based on the TH signals. The region of interest for TH terminals was created using Create Regions Around Objects function. The extent of colocalization was analyzed a built-in colocalization analysis module. The numbers of regions analyzed are indicated in the figure legends.

In situ hybridization was performed as previously described (Kasahara et al., 2021). Mice were deeply anesthetized with isoflurane and intracardially perfused with 10 ml of 4% paraformaldehyde (4% PFA) in PBS pH 7.4. After perfusion, the brains were quickly removed and stored in 4% PFA at 4°C overnight. The brains were cryoprotected with 10% sucrose for 2 h, 20% sucrose for 2 h, then 30% sucrose overnight, and embedded in OCT compound (Sakura Finetechnical). The striatum-containing brain regions were sliced at a 20 µm thickness. After post-fixing with 4% PFA for 10 min, the sections were treated for 30 min with proteinase K and subsequently acetylated in 0.45% acetic anhydride in triethylamine-HCl. The tissues were then hybridized overnight at 65°C in a solution containing digoxygenin (DIG)-labeled riboprobes as previously described (Kasahara et al., 2021, 2022; Masukawa et al., 2023). The sections were preincubated with PBS containing 10% bovine serum albumin and normal sheep serum for 90 min at room temperature and incubated with alkaline phosphatase-conjugated anti-DIG antibody overnight at 4°C. Specific signals were visualized using nitro-blue tetrazolium and 5-bromo-4-chloro-3′-indolyphosphate substrates. After in situ hybridization, the sections were blocked with 10% normal goat serum (NGS) in PBS with Tween 20 (pH7.4) at room temperature for 1 h. Reactions with the anti-ChAT antibody were performed at 4°C overnight. Sections were incubated with SignalStain® Boost IHC detection reagent (#8114, CST) for 30 min at room temperature. Bound probes were visualized with a 3,3′-diaminobenzidine tetrahydrochloride substrate kit (Vector Laboratories) at room temperature for 5–20 min. The antibody information is listed in Table 3.

To examine the protein-protein interaction between DRD2 and GPR143, we utilized a Duolink in situ proximity ligation assay (PLA) kit (Olink Bioscience) according to the manufacturer's protocol, as previously described (Masukawa et al., 2017, 2023). Specific signals were analyzed by confocal laser scanning microscopy (AX, Leica).

Table 3. Antibodies

Antibody	Company	Catalog Number	dilution IHC
TH	Millipore	AB152	1–1,000
TH	Immunostar	#22941	1–500
AADC	Kasahara et al. (2022)		1 µg/ml
GPR143	Fukuda et al. (2015)		1–500
DRD2	Frontier institute	D2R-Rb-Af960	1–500
DRD2(N-terminus)	Alomone Labs	ADR-002	1–500
DARPP32	GeneTex	GTX133350	1–500
ChAT	Millipore	AB144P	1–500
p-rpS6-Ser240/244	Cell Signaling	#2215	1–1,000

To confirm the AAV infection, mice were anesthetized with urethane (1.2 g/kg, i.p.) and fixed by perfusion with 4% PFA. Brains were quickly removed and fixed at 4°C for 16 h. Brain tissue was sectioned at a 50 µm thickness using a MicroSlicer Zero1 (Dosaka EM, Dosaka, Japan). Sections were permeabilized with Tris-buffered saline with 0.3% TritonX-100 (TBST) for 30 min at room temperature and blocked with TBST containing 10% NGS or normal horse serum for 1 h. The samples were then incubated with the primary antibodies listed in Table 3. Specific signals were visualized with Alexa Fluor donkey anti-rabbit IgG 488 and Alexa Flour donkey anti-goat IgG 594 antibodies (1:500) for 2 h at room temperature. The stained tissue was observed using an AX confocal microscope.

For quantitative analysis of phospho-S6 ribosomal protein ($Ser^{240/244}$) (p-rpS6-$Ser^{240/244}$), mice were fixed by perfusion with 4% PFA 75 min after the administration of haloperidol or saline. The brain sections were stained with primary antibodies against p-rpS6-$Ser^{240/244}$ and ChAT as described above. The mean intensity of p-rpS6-$Ser^{240/244}$ on ChAT was measured by Image J software.

Cell culture and immunocytochemistry. CHO cells stably expressing DRD2-mCherry were generated as previously described (Masukawa et al., 2023). Cells were cultured in F-12 Ham medium which was supplemented with 10% fetal bovine serum, penicillin (100 U/ml), and streptomycin (100 µg/ml). The cells were incubated at 37°C in a humidified atmosphere with 5% CO2 and used for the experiment within five passages. To determine whether the introduction of GPR143 alters the cell surface levels of DRD2 in CHO cells, we performed immunostaining using the anti-DRD2 N-terminus antibody listed in Table 3 without permeabilization. The CHO cells expressing DRD2-mCherry were plated at 3×10^4 cells in 8-well chamber slide glass. After overnight culture, the cells were transfected with 1 µg of *Gpr143-flag* or *free-flag* plasmids using Fugene6 (Promega), respectively. After 2 d of incubation, the cells were fixed with 4% PFA in PBS for 10 min and then incubated in PBS containing 10% NGS for 30 min. To examine the effect of L-DOPA on the cell surface expression of DRD2, the cells were pre-incubated with 10 nM L-DOPA for 10 min at room temperature. The cells were then fixed and incubated with the primary antibody. Specific signals were visualized with Alexa Fluor goat anti-rabbit IgG 488 antibody (1:500) for 2 h at room temperature. The stained cells were observed using an AX confocal microscope.

Electrophysiology. Mice (3–4 months old) were killed by decapitation under deep isoflurane anesthesia and coronal brain slices (300 µm) were cut using a microslicer (PRO-7, Dosaka) in ice-cold oxygenated cutting solution comprising the following (in mM): choline chloride, 92; KCl, 2.5; NaHCO3, 30; NaH_2PO_4, 1.2; HEPES, 20; D-glucose, 25; ascorbic acid, 5; thiourea, 2; sodium pyruvate, 3; N-acetyl-L-cysteine, 12; $CaCl_2$, 0.5; and $MgCl_2$, 10. The slices were transferred to a recovery chamber containing cutting solution at 31–32°C for 10 min. The slices were then incubated at room temperature in the holding chamber containing Krebs solution composing the following (in mM): NaCl, 124; KCl, 3; $NaHCO_3$, 26; NaH_2PO_4, 1; $CaCl_2$, 2.4; $MgCl_2$, 1.2; D-glucose, 10; and pH 7.4 when bubbled with 95% O_2 and 5% CO_2.

For recording, a brain slice was transferred to the recording chamber, submerged, and superfused with Krebs solution (bubbled with 95% O_2 and 5% CO_2, 32–34°C) at a rate of 2–3 ml/min. Cell-attached recordings were made on cholinergic interneurons using a patch clamp amplifier (Multiclamp 700B, Molecular Devices) to avoid attenuating intrinsic firing after breaking the membrane. Cholinergic interneurons were identified by their large somata under infrared-differential interference contrast microscopy using a 40× water immersion objective lens attached to an upright microscope (BX51WI, Olympus Optics). Images were detected with a charge-coupled device camera (IR-1000, DAGE-MTI) and displayed on a video monitor (VU-17, DAGE-MTI). In some recordings, a hyperpolarizing current was applied under the current clamp configuration after the experiments. All recorded neurons showed a voltage sag, which is a feature of cholinergic interneurons in the striatum. Recording patch pipettes were filled with potassium gluconate-based internal solution composing the following (in mM): potassium gluconate, 135; NaCl, 6; KCl, 10; K-HEPES, 10; Mg-ATP, 2; Na-GTP, 0.3; and K-EGTA, 0.1 (pH adjusted with 1 M KOH). To evoke DA release, a glass pipette filled with NaCl (1 M) was placed 100–200 µm from the recorded neuron and electrical stimulations (5 pulses delivered at 50 Hz) were delivered every 30 s. The stimulation intensity was set to evoke two to five postsynaptic currents in the recorded neuron during stimulation. The pause response was measured as the first inter-spike interval (ISI) ratio and pause time (Kharkwal et al., 2016). Briefly, the ISI ratio was calculated as the ratio of the ISI following stimulation versus the mean ISI during the baseline period before the stimulation. The pause time was calculated as the actual pause time (ISI between the last action potential during the stimulation period and the next action potential after the stimulation) minus the expected pause time (averaged ISI before stimulation).

Experimental design and statistical analyses. The investigators conducting the experiments were single-blinded to the mouse genotype. The sample size was arbitrarily set to between four and nine animals/group per experiment. For quantitative analysis of the immunohistochemical data, the fluorescence intensity of 10–30 neurons from each brain slice from five mice was calculated. For electrophysiologic analysis, one to two neurons were recorded from each brain slice, and three or four mice were used for each recording protocol. Data fitting and statistical analysis were performed using an unpaired Student's *t* test for comparisons between two groups and by two-way analysis of variance (ANOVA) for multiple groups, followed by Tukey's or Bonferroni's multiple comparison test using GraphPad Prism 9.5.1 (GraphPad). For analysis of the time-course experiment within 1 animal, repeated measures (RM) ANOVA was applied. A p value of less than 0.05 was considered statistically significant.

Results

Haloperidol-induced catalepsy was attenuated in *Gpr143*$^{-/y}$ mice

Cholinergic interneurons in the striatum receive synaptic inputs from midbrain DA neurons (Pickel and Chan, 1990; Dimova et al., 1993). We previously demonstrated that L-DOPA and DA are released from the striatum upon neural stimulation (Nakamura et al., 1993; Izawa et al., 2006). To identify L-DOPA-containing neurons, we first performed immunohistochemical analysis in the striatum and cerebral cortex using anti-TH and anti-AADC antibodies. TH and AADC expression were clearly higher in the dorsal striatum than in the cerebral cortex (Fig. 1*A–G*). While most TH-positive terminals lacked AADC signals in the cerebral cortex (Fig. 1*C,E*), most of those in the striatum showed intense AADC signals (Fig. 1*B,D*). However, a minor fraction of TH-positive terminals expressed AADC only moderately or weakly (Fig. 1*D*). AADC expression in TH-positive terminals was significantly higher in the striatum than in the cerebral cortex (Fig. 1*F*). Furthermore, when we measured the percentage of AADC-expression areas in TH-positive terminals comprised approximately 10% of the cerebral cortex. Thus, cortical neurons may mainly express TH but not AADC

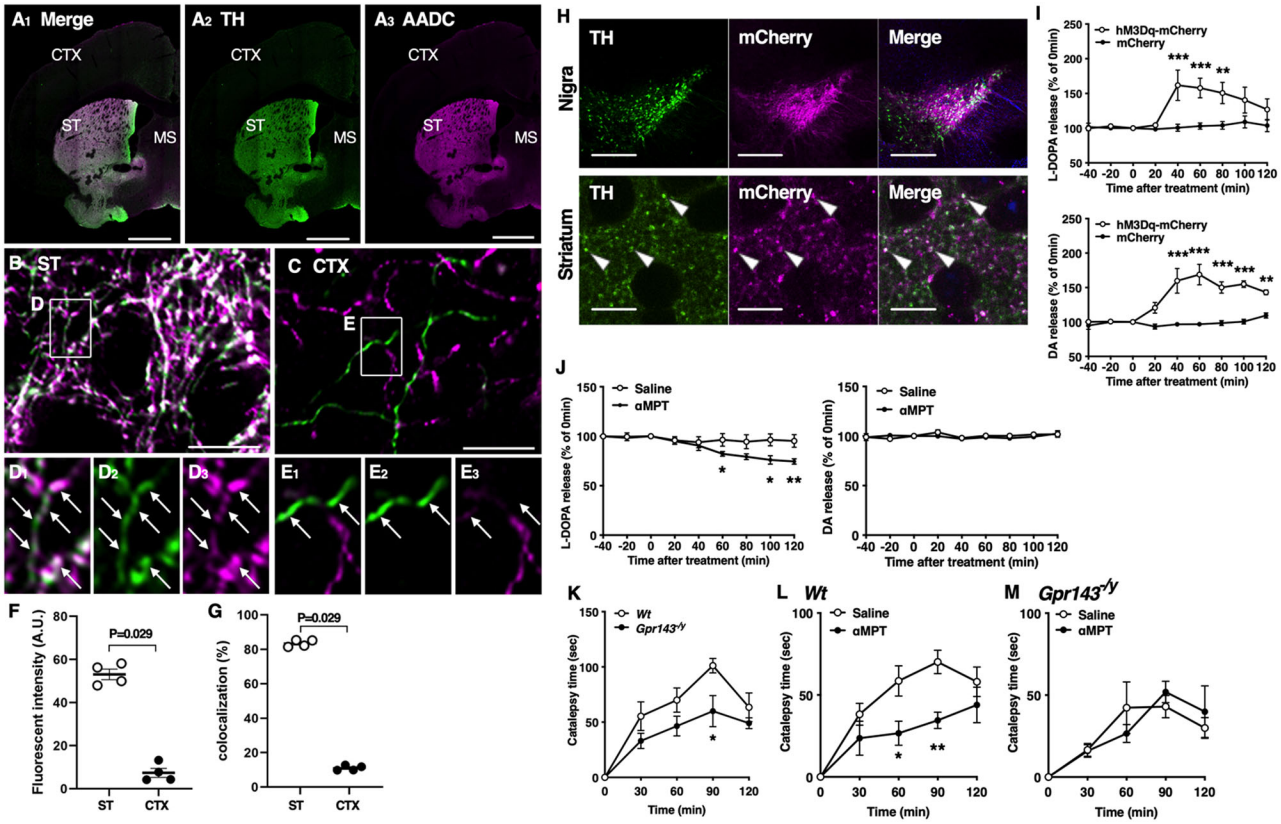

Figure 1. Presence and release of L-DOPA in the nigrostriatal dopaminergic neurons. ***A–E***, Double immunofluorescence showing the expression of TH (green) and AADC (magenta) protein in the cerebral cortex (CTX) and striatum (ST). Enclosed region in B (ST) and C (CTX) is magnified (in *D*) and E, respectively. Arrows indicate TH-positive varicosities. ***D***, Note that although most TH-positive terminals show intense AADC signals, some of them show only weak signals in the ST. Scale bar, 1 mm in A; 10 µm (in ***B, C***). ***F***, Quantitative analysis showing the fluorescence intensity of AADC in TH-positive terminals. Note that AADC expression is significantly higher in ST than in CTX ($n = 4$, Mann–Whitney *U* test). ***G***, Quantitative analysis showing the percentage of AADC-expressing regions in TH-positive regions. In ST, intense AADC signals are detected in most but not all TH-positive regions ($n = 4$, Mann–Whitney *U* test). ***H***, TH (green) and mCherry (magenta) signals in the substantia nigra (upper) and dorsolateral striatum (lower) of *Dat-cre* mice after infection with AAV2/1-DIO-hM3Dq-mCherry. Arrowheads indicate colocalization of TH and mCherry. Scale bars, 200 and 10 µm in the substantia nigra and striatum, respectively. ***I***, L-DOPA (upper) and DA (lower) release from the dorsolateral striatum before and after treatment with clozapine-N-oxide (3 mg/kg, i.p.) in *Dat-cre* mice infected with AAV2/1-DIO-hM$_3$Dq-mCherry (hM$_3$Dq-mCherry) or -mCherry in the substantia nigra (drug, $F_{(1,6)} = 6.496$, $p = 0.044$, time, $F_{(8,48)} = 6.732$, $p < 0.0001$, drug × time, $p < 0.001$ for L-DOPA and drug, $F_{(1,6)} = 34.91$, $p = 0.001$, time, $F_{(8,48)} = 13.04$, $p < 0.0001$, drug × time, $F_{(8,48)} = 12.08$, $p < 0.0001$ for DA, $n = 5$). ***J***, L-DOPA (left) and DA (right) release before and after treatment with αMPT (3 mg/kg, i.p.) or saline in the dorsolateral striatum of Wt mice (drug, $F_{(1,8)} = 12.54$, $p = 0.008$, time, $F_{(2.891,23.13)} = 16.77$, $p < 0.001$, drug × time, $p < 0.001$ for L-DOPA and drug, $F_{(1,8)} = 0.353$, $p = 0.569$, time, $F_{(3.833,\ 30.66)} = 1.302$, $p = 0.292$, drug × time, $p = 0.715$ for DA, $n = 5$). ***K, L, M***, Decrease in the L-DOPA release attenuates haloperidol-induced catalepsy through GPR143. ***K***, Time course of catalepsy after treatment with haloperidol (0.5 mg/kg) in Wt and *Gpr143*$^{-/y}$ mice ($F_{(1,10)} = 7.368$, $p = 0.022$, $n = 6$). ***L, M***, Time course of haloperidol-induced catalepsy after treatment with αMPT. αMPT (3 mg/kg) was applied simultaneously with haloperidol in (***L***) Wt (saline/haloperidol, $F_{(1,16)} = 7.938$, $p = 0.047$, $n = 9$) and (***M***) *Gpr143*$^{-/y}$ mice (saline/haloperidol, $F_{(1,10)} = 0.005$, $p = 0.943$, $n = 6$). All values are the mean ± standard error of the mean. *$P < 0.05$, **$p < 0.01$, ***$p < 0.001$, two-way ANOVA with Bonferroni's multiple comparisons test.

and may contain L-DOPA as an endproduct, the consistent finding with a previous report (Ikemoto et al., 1999). In clear contrast, the AADC-expression areas in TH-positive terminals comprised approximately 80% of the striatum; the remaining ∼20% of the regions lacked strong AADC expression (Fig. 1*G*). Therefore, a minority of TH-positive terminals in the striatum did not show intense AADC signals. Regardless of AADC expression, L-DOPA is likely to be released from TH-positive neurons as L-DOPA is synthesized by TH. To test this possibility, we next applied the DREADD system to the *Dat-cre* mice using AAV2/1 encoding DIO-hM3Dq-mCherry and DIO-mCherry. We confirmed that hM3Dq-mCherry fluorescence was present in the substantia nigra and dorsolateral striatum. The signals were colocalized with TH-immunoreactive cells (Fig 1*H*). In hM3Dq-mCherry-expressing mice, administration of CNO (3 mg/kg, i.p.) increased the release of L-DOPA and DA from the dorsolateral striatum. Neither L-DOPA nor DA was released upon the administration of CNO in mCherry-expressing mice [repeated measures (RM), two-way ANOVA, drug; $F_{(1,6)} = 6.496$, $p = 0.044$ for L-DOPA, $F_{(1,6)} = 34.91$, $p = 0.001$ for DA, Fig. 1*I*). These results indicate that endogenous L-DOPA was released from TH-positive nigro-striatal dopaminergic neurons. A high dose of αMPT decreased both DA and L-DOPA release from rat striatum (Nakamura et al., 1993). Consistently, αMPT at a high dose (200 mg/kg, i.p.) decreased both L-DOPA and DA release from the dorsal striatum to 35.7% and 31.3%, respectively. As previously observed, a low dose of αMPT (3 mg/kg, i.p.) decreased the L-DOPA release without affecting the DA release (RM, two-way ANOVA, drug; $F_{(1,8)} = 12.54$, $p = 0.008$ for L-DOPA, $F_{(1,8)} = 0.353$, $p = 0.569$ for DA, Fig. 1*J*) (Masukawa et al., 2023). To determine whether endogenous L-DOPA is involved in haloperidol-induced catalepsy, we examined the catalepsy time in Wt and *Gpr143*$^{-/y}$ mice treated with haloperidol (0.5 mg/kg, i.p.) with or without αMPT (3 mg/kg, i.p.) pretreatment. Haloperidol markedly increased the catalepsy time in Wt mice. The effect of haloperidol was attenuated in *Gpr143*$^{-/y}$

mice (RM, two-way ANOVA, genotype; $F_{(1,10)} = 7.368$, $p = 0.021$, Fig. 1*K*). Pre-treatment with αMPT attenuated haloperidol-induced catalepsy in Wt mice (RM, two-way ANOVA; $F_{(1,16)} = 7.938$, $p = 0.012$, Fig. 1*L*). Moreover, the effect of αMPT was not observed in *Gpr143*$^{-/y}$ mice (RM, two-way ANOVA, $F_{(1,10)} = 0.005$, $p = 0.943$, Fig. 1*M*). These findings suggest that endogenous L-DOPA released from the dorsolateral striatum modulates haloperidol-induced catalepsy through GPR143. Together, our findings suggest that L-DOPA released upon excitation of the nigro-striatal dopaminergic neurons is involved in haloperidol-induced catalepsy through GPR143.

Coupling between GPR143 and DRD2 in haloperidol-induced catalepsy

We recently demonstrated that L-DOPA enhances the coupling between GPR143 and DRD2 and potentiates the behavioral response to quinpirole. We identified the TM5 domain of GPR143 as the region that interacts with DRD2. The responsiveness to quinpirole is attenuated by disrupting the interaction between GPR143 and DRD2 using a human immunodeficiency virus TAT peptide fused with the TM5 of GPR143 (TAT-TM5) (Masukawa et al., 2023). In the present study, we tested the effect of TAT-TM5 to examine whether a similar mechanism is involved in haloperidol-induced catalepsy. With an in situ PLA assay, GPR143-DRD2 protein-protein interaction signals were observed in the dorsolateral striatum of Wt mice but not *Gpr143*$^{-/y}$ mice (Fig. 2*A,B*). TAT-TM5 (100 pmol, i.c.v.) inhibited the interaction signals compared with TAT-control (unpaired *t* test, $p = 0.012$, Fig. 2*C*). Importantly, TAT-TM5 alone did not produce catalepsy in mice (data not shown). TAT-TM5 attenuated the haloperidol-induced catalepsy compared with the TAT-control (RM, two-way ANOVA, $F_{(1,10)} = 7.358$, $p = 0.022$, Fig. 2*D*). The effect of TAT-TM5 was not observed in *Gpr143*$^{-/y}$ mice (RM, two-way ANOVA, $F_{(1,9)} = 0.018$, $p = 0.897$, Fig. 2*E*). These results suggest that coupling between GPR143 and DRD2 modulates haloperidol-induced catalepsy.

GPR143 in cholinergic interneurons of the dorsal striatum modulates haloperidol-induced catalepsy

We next attempted to identify the neural circuits responsible for the phenotypic defect in *Gpr143*$^{-/y}$ mice. For this purpose, we assessed haloperidol-induced catalepsy in mice expressing cre recombinase in DRD2-, ChAT (cholinergic interneuron)-, and ADORA2A (indirect pathway)-positive neurons. Attenuation of haloperidol-induced catalepsy was observed in *Drd2-cre*(+); *Gpr143*$^{flox/y}$ mice and *ChAT-cre;Gpr143*$^{flox/y}$ mice but not in *Adora2a-cre; Gpr143*$^{flox/y}$ mice compared with corresponding control mice (RM, two-way ANOVA, genotype; $F_{(1,14)} = 7.753$, $p = 0.015$ for *Drd2-cre,* $F_{(1,14)} = 5.064$, $p = 0.0410$ for *ChAT-cre,* $F_{(1,12)} = 0.058$, $p = 0.814$ for *Adora2a-cre*, Fig. 3*A–C*). We confirmed that *Gpr143* mRNA signals colocalized with ChAT-immunoreactive signals in the dorsolateral striatum (Fig. 3*D,E*). These findings suggest that GPR143 expressed in cholinergic interneurons of the dorsal striatum is involved in haloperidol-induced catalepsy.

To examine the specificity as a loss of function of GPR143, we performed re-expression analysis of GPR143 using AAVdj encoding GPR143-P2A-EGFP or EGFP in the dorsal striatum of *Gpr143*$^{-/y}$ mice (Fig. 4*A*). We confirmed that EGFP signals were observed in the dorsal striatum. GPR143-P2A-EGFP signals were colocalized with ChAT-positive signals in neurons in the

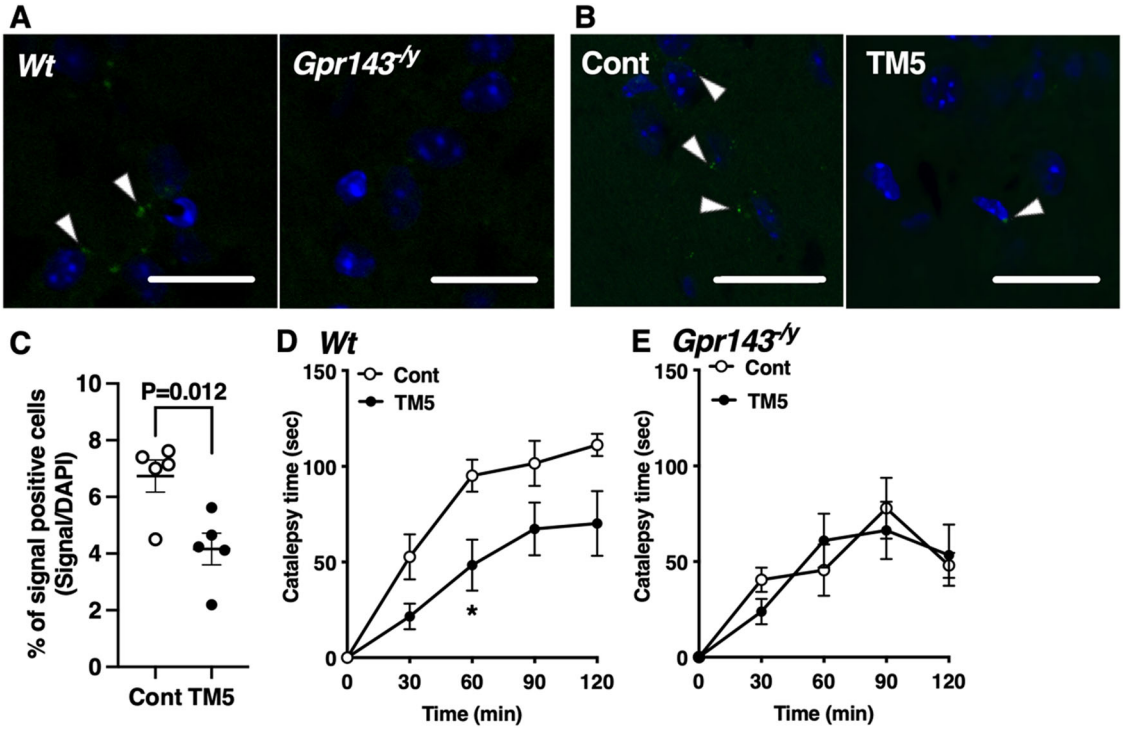

Figure 2. TAT-TM5 peptide inhibits haloperidol-induced catalepsy. ***A***, Interaction signals between GPR143 and DRD2 were observed in the dorsolateral striatum of Wt but not *Gpr143*$^{-/y}$ mice (left). ***B***, The effect of TAT-control (Cont) or TAT-TM5 (TM5) (100 pmol, i.c.v) on interaction signals between GPR143 and DRD2 in the dorsolateral striatum of Wt mice. Scale bar, 20 µm. Blue signals stained with 4′,6-diamidino-2-phenylindole. ***C***, Data are shown as the percentage of in situ PLA signal-positive cells in the dorsal striatum ($n = 6$ animals). ***D, E***, Effect of pre-treatment with TM5 or Cont (100 pmol, i.c.v) on haloperidol-induced catalepsy in Wt (***D***) and *Gpr143*$^{-/y}$ (***E***) mice ($F_{(1,10)} = 7.358$, $p = 0.022$ in Wt, $F_{(1,9)} = 0.018$, $p = 0.8973$ in *Gpr143*$^{-/y}$). *$P < 0.05$, two-way ANOVA with Tukey's multiple comparisons test. All values are the mean ± standard error of the mean.

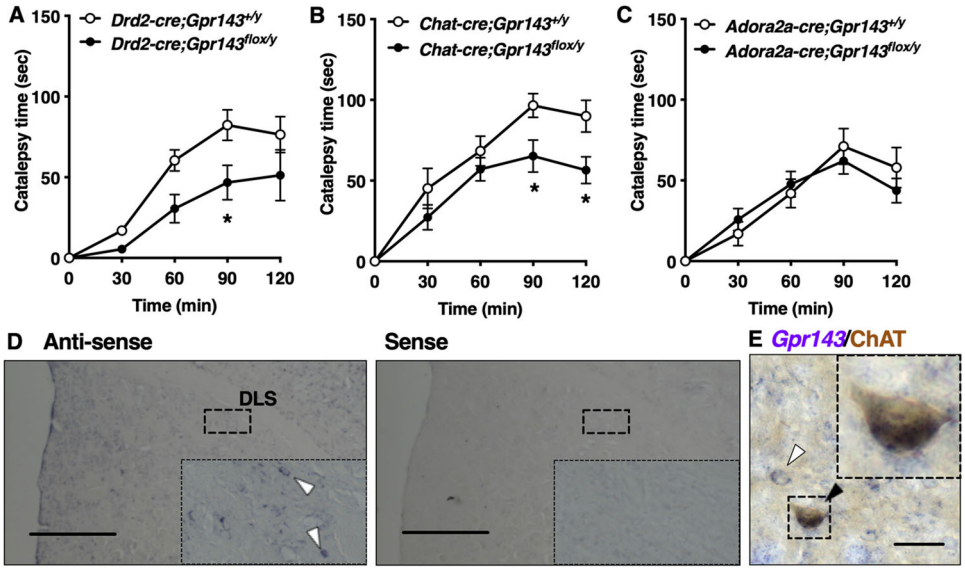

Figure 3. Haloperidol-induced catalepsy is attenuated in *DRD2-cre (+); Gpr143$^{flox/y}$* mice and *ChAT-cre (+); Gpr143$^{flox/y}$* mice. ***A–C***, Time course of catalepsy after treatment with haloperidol in (***A***) *Drd2-cre(+);Gpr143$^{flox/y}$*, (***B***) *ChAT-cre; Gpr143$^{flox/y}$*, and (***C***) *Adora2a-cre; Gpr143$^{flox/y}$* mice and corresponding control mice ($F_{(1,14)} = 7.753$, $p = 0.015$ in *Drd2-cre;Gpr143$^{flox/y}$*, $F_{(1,14)} = 5.064$, $p = 0.041$ in *ChAT-cre; Gpr143$^{flox/y}$*, $F_{(1,12)} = 0.058$, $p = 0.814$ in *Adora2a-cre; Gpr143$^{flox/y}$*, $n = 6–9$). $^*P < 0.05$, $^{**}p < 0.01$, two-way ANOVA with Tukey's multiple comparisons test. All values are the mean ± standard error of the mean. ***D***, In situ hybridization signals for *Gpr143* mRNA using anti-sense (left) and sense (right) probes in the dorsal striatum. Scale bar, 500 µm. Boxed areas indicate magnified images. ***E***, *Gpr143* mRNA (purple) and ChAT immunoreactive (brown) signals in the dorsolateral striatum of a Wt mouse. Black and white arrowheads indicate *Gpr143*-positive/ChAT-positive and *Gpr143*-positive/ChAT-negative neurons, respectively. Boxed areas indicate magnified images. Scale bar, 30 µm.

dorsal striatum of mice injected with AAVdj (Fig. 4*B*). Re-expression of GPR143-P2A-EGFP in the dorsal striatum of *Gpr143$^{-/y}$* mice rescued the impaired behavioral response to haloperidol compared with the EGFP-expressing mice (RM, two-way ANOVA, $F_{(1,15)} = 6.863$, $p = 0.019$, Fig. 4*C*). We further performed neuron-specific re-expression analysis of GPR143 in ChAT-positive neurons of the dorsal striatum using AAV9-DIO-GPR143-P2A-EGFP or AAV9-DIO-EGFP. EGFP signals colocalized with ChAT-positive signals in neurons in the dorsal striatum of *Drd2-cre;Gpr143$^{-/y}$* mice (Fig. 4*B*). Re-expression of GPR143-P2A-EGFP in DRD2-positive neurons prolonged the haloperidol-induced catalepsy time compared with EGFP-expressing mice (RM, two-way ANOVA, $F_{(1,10)} = 8.611$, $p = 0.015$, Fig. 4*D*). In *ChAT-cre;Gpr143$^{-/y}$* mice, EGFP signals were observed in ChAT-positive neurons in the dorsal striatum (Fig. 4*B*). Re-expression of GPR143-P2A-EGFP in cholinergic interneurons in *ChAT-cre;Gpr143$^{-/y}$* mice also prolonged the haloperidol-induced catalepsy time compared with than in EGFP-expressing mice (RM, two-way ANOVA, $F_{(1,11)} = 17.94$, $p = 0.001$, Fig. 4*E*). These observations further suggest that GPR143 expressed in cholinergic interneurons of the dorsal striatum positively modulates the function of DRD2 that mediates haloperidol-induced catalepsy.

GPR143 modulates single-cell DRD2-mediated responses in cholinergic interneurons

Haloperidol promotes rpS6 phosphorylation at the Ser$^{240/244}$ residue (p-rpS6-Ser$^{240/244}$) in the dorsolateral striatum, and this effect is attenuated by ablating DRD2 in cholinergic interneurons (Kharkwal et al., 2016). The levels of p-rpS6-Ser$^{240/244}$ parallel the state of physiologic activities of striatal cholinergic interneurons (Bertran-Gonzalez et al., 2012). Consistent with previous report, haloperidol increased the fluorescence intensity of p-rpS6-Ser$^{240/244}$ in the dorsolateral striatum of *ChAT-cre;Gpr143$^{+/y}$* mice. To elucidate the role of GPR143 in the downstream signaling events of DRD2 in cholinergic interneurons, we examined the effect of haloperidol in *ChAT-cre;Gpr143$^{flox/y}$* mice. As expected, the haloperidol-induced rpS6-Ser$^{240/244}$ phosphorylation was attenuated in *ChAT-cre;Gpr143$^{flox/y}$* mice compared with *ChAT-cre;Gpr143$^{+/y}$* mice (RM, two-way ANOVA, $F_{(1,357)} = 8.338$, $p = 0.004$, Fig. 5*B*).

It is possible that the GPR143-DRD2 interaction stabilizes the pool of DRD2 available to be stimulated by extracellular DA. We examined cell surface levels of DRD2 in the CHO cells co-expressing both DRD2-mCherry and GPR143-flag or DRD2-mCherry alone after pre-treatment with L-DOPA or with control buffer. The levels of DRD2-mCherry fluorescence, indicating the total levels of DRD2, were similar in both the CHO cells expressing DRD2-mCherry alone and CHO cells co-expressing DRD2-mCherry and GPR143-flag (Fig. 6). The cell surface levels of DRD2, however, were higher in CHO cells co-expressing DRD2 and GPR143 than in cells expressing DRD2 alone. L-DOPA increased the cell surface levels of DRD2 in CHO cells co-expressing DRD2 and GPR143 but not in cells expressing DRD2 alone (two-way ANOVA, Mock/GPR143: $F_{(1,28)} = 0.304$, $p = 0.586$; drug: $F_{(1,28)} = 0.015$, $p = 0.904$; Mock/GPR143×drug: $F_{(1,28)} = 0.025$, $p = 0.875$ for total; Mock/GPR143: $F_{(1,28)} = 39.04$, $p < 0.001$; drug: $F_{(1,28)} = 8.590$, $p = 0.007$; Mock/GPR143×drug: $F_{(1,28)} = 4.593$, $p = 0.041$ for cell surface, Fig. 6*B*). This result suggests that L-DOPA/GPR143 signaling enhanced cell surface levels of DRD2 that can be blocked by haloperidol.

To further examine the role of GPR143 at the single-cell level, we performed cell-attached recordings of cholinergic interneurons in coronal brain slices from adult *ChAT-cre;Gpr143$^{+/y}$* and *ChAT-cre;Gpr143$^{flox/y}$* mice. Cholinergic interneurons spontaneously fired (Fig. 7*A*). The firing rates were not different between *ChAT-cre;Gpr143$^{+/y}$* and *ChAT-cre;Gpr143$^{flox/y}$* mice ($t_{(15)} = -0.69$, Fig. 7*B*), indicating that the intrinsic firing properties were not affected in *ChAT-cre;Gpr143$^{flox/y}$* mice. Previous studies described a "pause" in the firing of cholinergic interneurons that

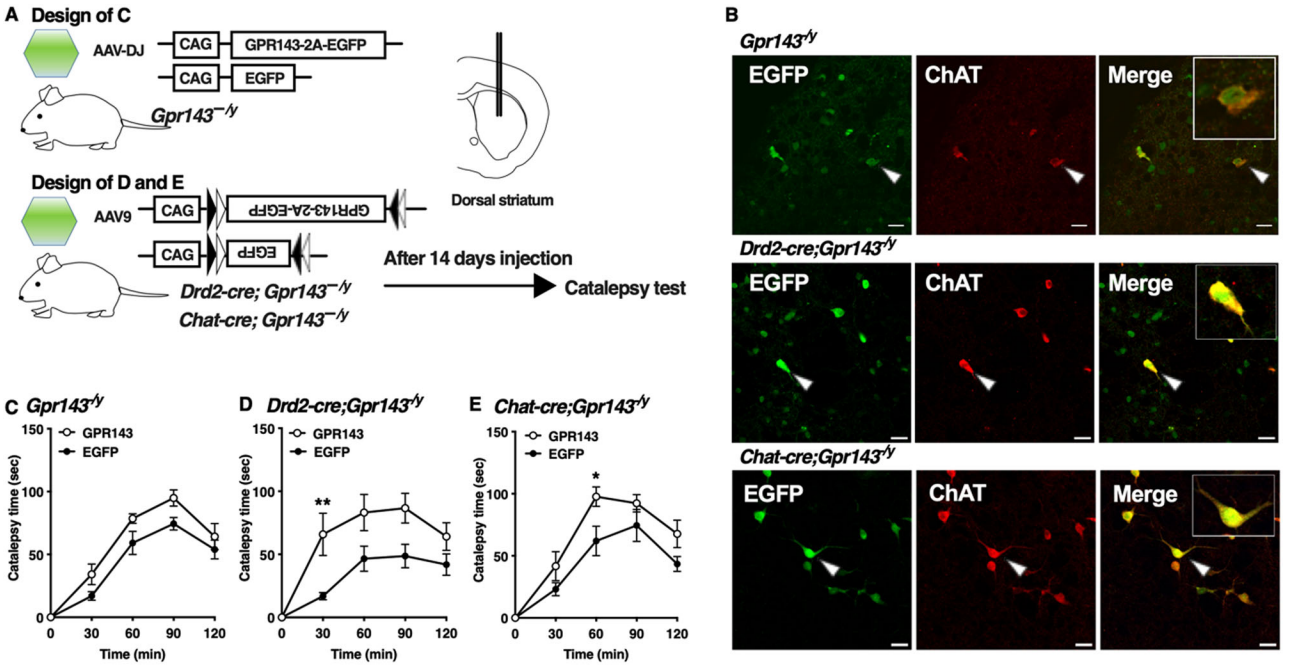

Figure 4. Re-expression of GPR143 in cholinergic interneurons of the dorsal striatum prolongs haloperidol-induced catalepsy. ***A***, Experimental design of the rescue of GPR143. ***B***, EGFP (green), ChAT (red), and merged signals in the dorsolateral striatum of *Gpr143*$^{-/y}$ (upper), *Drd2-cre;Gpr143*$^{-/y}$ (middle), and *ChAT-cre;Gpr143*$^{-/y}$ (lower) mice infected with AAV-DJ-GPR143-P2A-EGFP or AAV9-DIO-GPR143-P2A-EGFP. The EGFP signals (arrowhead) were merged with ChAT-positive signal. Scale bar, 30 µm. ***C***, Time course of catalepsy after treatment with haloperidol in *Gpr143*$^{-/y}$ mice infected with AAV-DJ-GPR143-P2A-EGFP (GPR143) or -EGFP in the dorsal striatum ($F_{(1,15)} = 6.863$, $p = 0.019$, $n = 8\sim9$). ***D, E***, Time course of catalepsy after treatment with haloperidol in "(***D***) *Drd2-cre;Gpr143*$^{-/y}$ and (***E***) *Chat-cre; Gpr143*$^{-/y}$ mice infected with AAV9-DIO-GPR143-P2A-EGFP (GPR143) or DIO-EGFP in the dorsal striatum. ($F_{(1,10)} = 8.611$, $p = 0.015$ in *Drd2-cre; Gpr143*$^{-/y}$, $F_{(1,11)} = 17.94$, $p = 0.001$ in *ChAT-cre; Gpr143*$^{-/y}$, $n = 6$–7). *$P < 0.05$,**$p < 0.01$, two-way ANOVA with Bonferroni's multiple comparisons test. All values are the mean ± standard error of the mean. n.s. indicates not significant.

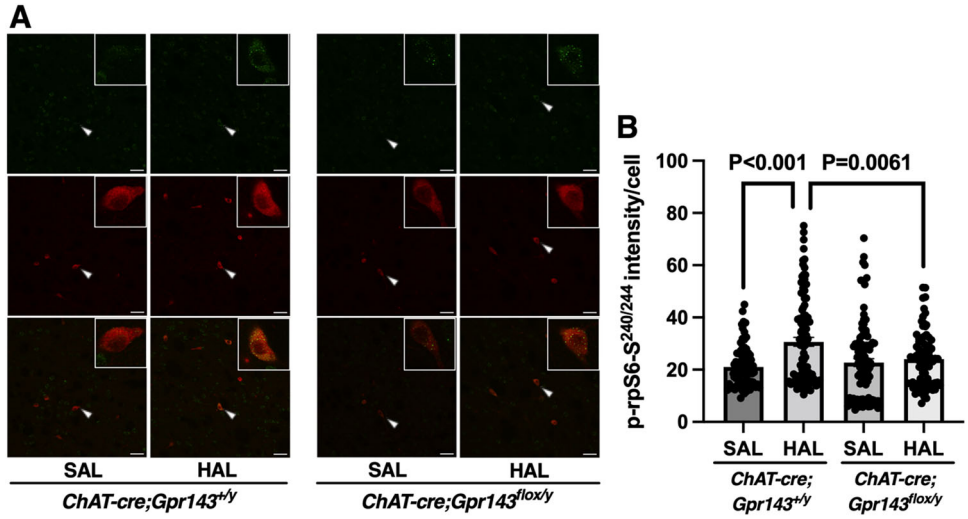

Figure 5. Phosphorylation of rpS6 at the Ser$^{240/244}$ residue by haloperidol is attenuated in *Chat-cre;Gpr143*$^{flox/y}$ mice. ***A***, Immunostaining images of p-rpS6-Ser$^{240/244}$ (green) and ChAT (red) after treatment with haloperidol or saline in the dorsolateral striatum of *Chat-cre;Gpr143*$^{+/y}$ and *Chat-cre;Gpr143*$^{flox/y}$ mice. Arrowheads indicate p-rpS6-Ser$^{240/244}$ signal in ChAT-positive cells. Scale bar, 50 µm. ***B***, Quantitative analysis of p-rpS6-Ser$^{240/244}$ immunofluorescence is shown as the fluorescence intensity of p-rpS6-Ser$^{240/244}$ on ChAT-positive neurons (drug, $F_{(1,357)} = 14.79$, $p < 0.0001$, genotype, $F_{(1,357)} = 3.055$, $p = 0.081$, drug × genotype, $F_{(1,357)} = 8.338$, $p < 0.004$, $n = 79$–104 cells, $n = 5$ animals). All values are the mean ± standard error of the mean. Statistical significance was determined using a two-way ANOVA with Tukey's multiple comparisons test.

was attenuated in mice lacking DRD2 in the cholinergic interneurons (Kharkwal et al., 2016). Thus, this response is mediated by DRD2 (Aosaki et al., 1994; Straub et al., 2014) although the synaptic and cellular mechanisms are not entirely understood. We compared the pause in two ways as previously described (Kharkwal et al., 2016, see methods). In *ChAT-cre;Gpr143*$^{+/y}$ slices, the pause was 378.8 ± 95.1 ms (Fig. 7*D*, 8 neurons from 4 mice) and the ISI ratio was 2.84 ± 0.28 (Fig. 7*E*). In *ChAT-cre;Gpr143*$^{flox/y}$ slices, the pause duration and ISI ratio were significantly attenuated compared with *ChAT-cre; Gpr143*$^{+/y}$ (pause:−125 ± 110.3 ms, 9 neurons from 3 mice, $t_{(15)} = 3.42$, $p = 0.004$, ISI ratio:1.1 ± 0.33, 9 neurons from 3 mice,

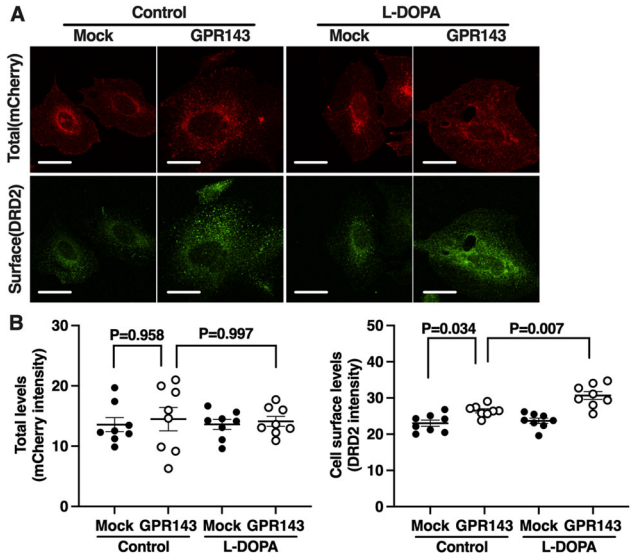

Figure 6. L-DOPA enhances the cell surface level of DRD2 in CHO cells co-expressing DRD2 and GPR143. ***A***, Expression levels of mCherry (total DRD2, red) and DRD2 (cell surface DRD2, green) in the CHO cells expressing both DRD2-mCherry and mock vector or DRD2-mCherry and GPR143-flag after treatment with L-DOPA (10 nM) or control buffer. Scale bar, 10 µm. ***B***, Quantitative analysis of mCherry and DRD2 immunofluorescence is shown by each fluorescence intensity ($n = 8$ cell culture preparations). All values are the mean ± standard error of the mean. Statistical significance was determined using a two-way ANOVA with Tukey's multiple comparisons test.

$t_{(15)} = 3.1$, $p = 0.007$, respectively). These findings indicate that GPR143 positively regulates the DRD2-mediated synaptic response in cholinergic interneurons.

Discussion

GPR143 expressed in cholinergic interneurons is involved in haloperidol-induced catalepsy

DRD2-mediated signaling plays a critical role in regulating the activity of striatal cholinergic interneurons and in the mechanisms of typical antipsychotic side effects (Kharkwal et al., 2016). In the present study, we examined which neural circuits expressing the L-DOPA receptor GPR143 are involved in dopaminergic transmission. Using haloperidol as a probe, we found that coupling between DRD2 and GPR143 modulates DRD2-mediated dopaminergic transmission in cholinergic interneurons (Figs. 2–4). Reducing the endogenous release of L-DOPA and preventing interactions between GPR143 and DRD2 suppresses haloperidol-induced catalepsy in Wt mice but not in *Gpr143*$^{-/y}$ mice (Fig. 1*K*,*L*,*H*). Administration of haloperidol increased the phosphorylation levels of rpS6 at Ser240/244, a downstream signaling molecule initiated by DRD2 activation, in the dorsolateral striatum of Wt mice, but this increase was not observed in *Chat-cre;Gpr143*$^{flox/y}$ mice (Fig. 5). Introduction of GPR143 increased the cell surface levels of DRD2 in CHO cells expressing DRD2. L-DOPA further enhanced DRD2 cell surface expression in CHO cells co-expressing DRD2 and GPR143 (Fig. 6). Shorter pauses in cholinergic interneuron firing activity were observed after intrastriatal stimulation in striatal slices from *Chat-cre;Gpr143*$^{flox/y}$ mice compared with Wt mice (Fig. 7). These findings provide the first evidence for a modulatory role of the L-DOPA receptor GPR143 in DRD2-mediated signaling in a single cell of the defined neural circuit, the cholinergic interneurons.

Using the DREADD system, we demonstrated here that selective stimulation of TH-positive nigrostriatal dopaminergic neurons elicited the release of L-DOPA from the dorsolateral striatum (Fig. 1*I*). Although the presence of L-DOPA-containing vesicles is unknown (Tison et al., 1989; Karasawa et al., 1992), this finding clearly shows that L-DOPA and DA were released from TH-positive nigrostriatal DA neurons. Is L-DOPA thus endogenously released modify haloperidol-induced catalepsy? Several lines of evidence suggest that L-DOPA is a ligand for GPR143 (Lopez et al., 2008; Goshima et al., 2019). L-DOPA sensitizes vasomotor tone through modulating vascular adrenergic α_1 receptor (ADRA1) via GPR143 (Masukawa et al., 2017). L-DOPA induces hippocampal neurogenesis via GPR143, and these actions of L-DOPA are not mimicked by dopamine and are not observed in cells derived from *Gpr143*$^{-/y}$ mice (Kasahara et al., 2022). In this study, we utilized a low dose of αMPT, a competitive TH inhibitor that selectively modifies the release of L-DOPA without changing the DA release (Nakamura et al., 1993; Masukawa et al., 2023), since L-DOPA ester compound L-DOPA cyclohexyl ester, an antagonist against GPR143 is readily converted to L-DOPA in living cells and can only be effective within a certain period of time (Misu et al., 1996; Furukawa et al., 2000). We showed that the αMPT administration attenuated haloperidol-induced catalepsy (Fig. 1*L*), as did loss of GPR143 (Fig. 1*K*). The effect of αMPT was not observed in *Gpr143*$^{-/y}$ mice (Fig. 1*M*). In addition, L-DOPA increased the cell surface level of DRD2 in CHO cells co-expressing DRD2 and GPR143 (Fig. 6). Although further studies are required to elucidate the underlying mechanisms, these findings together support the idea that L-DOPA released coincident with neuronal activity may positively regulate DRD2 signaling through GPR143, thereby potentiating haloperidol-induced catalepsy.

DRD2 signaling through coupling between GPR143 and DRD2

We recently reported that L-DOPA potentiates DRD2 signaling through GPR143 (Masukawa et al., 2023). GPR143 interacts with DRD2 at the TM5 domain, and L-DOPA enhances this interaction. TAT-TM5 peptide, which hinders the interaction between GPR143 and DRD2, mitigates the locomotor effects of quinpirole (Masukawa et al., 2023). Likewise, pre-treatment with the TAT-TM5 peptide attenuates haloperidol-induced catalepsy (Fig. 2). These findings suggest a functional coupling between GPR143 and DRD2 in cholinergic interneurons. We also observed that GPR143 potentiates ADRA1B-mediated downstream signaling by forming a heteromeric complex with ADRA1B. L-DOPA augments this heteromerization and ADRA1B-mediated phenylephrine-induced Ca^{2+} mobilization (Masukawa et al., 2017). GPR143 may couple with several GPCRs and modifies signaling mediated by these GPCRs. Importantly, however, even though DRD1 and DRD3 physically interact with GPR143, L-DOPA does not enhance the interactions between GPR143 and DRD1 or DRD3 (Masukawa et al., 2023). The structural basis for such a selective interaction of GPR143 and other GPCRs is unknown. Further studies are required to delineate the structural basis of the ligand-dependent functional coupling between GPR143 and DRD2.

Neural circuits in which functional coupling between DRD2 and GPR143 occurs

The phenotypic defect in *Gpr143*$^{-/y}$ was observed in both *Drd2-cre;Gpr143*$^{flox/y}$ mice and *ChAT-cre;Gpr143*$^{flox/y}$ mice. Consistent with

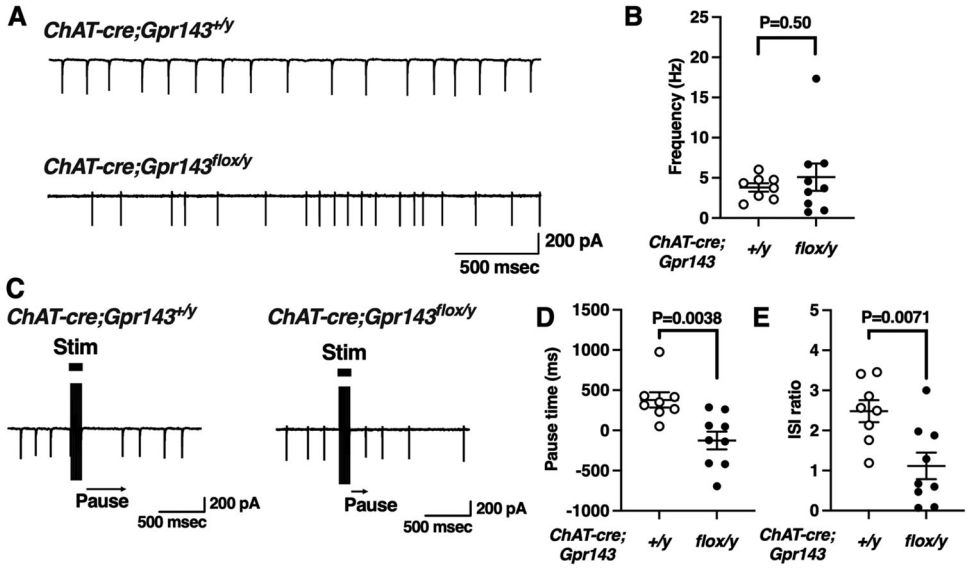

Figure 7. Reduction of the cholinergic interneuron "Pause" in *Chat-cre;Gpr143$^{flox/y}$ mice*. ***A***, Typical trace of cell-attached firing rates in neurons from *Chat-cre;Gpr143$^{+/y}$* and *Chat-cre;Gpr143$^{flox/y}$* mouse slices. ***B***, Summary of average cell-attached firing rates in neurons from *Chat-cre;Gpr143$^{+/y}$* and *Chat-cre;Gpr143$^{flox/y}$* mouse slices ($n = 8$ and $9/n = 4$ and 3 mice). ***C***, Representative responses in cholinergic interneurons elicited by intrastriatal electrical stimulation. Cells were recorded in the whole-cell current-clamp configuration from *Chat-cre;Gpr143$^{+/y}$* and *Chat-cre;Gpr143$^{flox/y}$* slices, which fired additional action potentials in response to intrastriatal electrical stimulation. ***D***, Summary of average pause in firing, expressed as the actual pause minus the expected pause (based on the ISIs in the pre-stimulation period), in *Chat-cre;Gpr143$^{+/y}$* and *Chat-cre;Gpr143$^{flox/y}$* slices ($n = 8$ and $9/n = 4$ and 3 mice). ***E***, Summary of average pause, expressed as the ratio of the first ISI to the average (pre-stimulation) ISI, in *Chat-cre;Gpr143$^{+/y}$* and *Chat-cre;Gpr143$^{flox/y}$* slices. All values are the mean ± standard error of the mean. Statistical significance was determined using Student's *t* test.

this, haloperidol-induced catalepsy is attenuated following the deletion of DRD2 from cholinergic interneurons (Kharkwal et al., 2016). Haloperidol-induced catalepsy is thought to be due to the activation of iMSNs via acetylcholine M1 receptors by increased levels of acetylcholine resulting from the antagonism of DRD2 on cholinergic interneurons. Haloperidol increased the phosphorylation of rpS6 at Ser$^{240/244}$ in cholinergic interneurons in the dorsolateral striatum. This action of haloperidol was not observed in *Chat-cre;Gpr143$^{flox/y}$* mice, indicating that the cholinergic tone is lower in *Chat-cre;Gpr143$^{flox/y}$* mice than in Wt mice, consistent with a previous finding that rpS6 signaling is dampened in *Chat-cre; DRD2^{flox}* mice (Kharkwal et al., 2016). Together, these findings suggest that GPR143 co-expressed with DRD2 in cholinergic interneurons modulates DRD2 function, thereby mediating haloperidol-induced catalepsy.

Our recent study suggests that GPR143 regulates neurogenesis, neural development, and maturation in the hippocampus (Kasahara et al., 2022). It may be possible that loss of the *Gpr143* gene lead to abnormal development and maturation in the striatal local circuitry. In our re-expression experiment, however, the phenotypic defect in *Gpr143$^{-/y}$* mice was rescued by re-expression of GPR143 in cholinergic interneurons of the dorsolateral striatum. Spontaneous firing in cholinergic interneurons did not differ between Wt and *Gpr143$^{-/y}$* mice (Fig. 7). These findings suggest that GPR143 on striatal cholinergic interneurons regulates DRD2 function.

GPR143 as a potential drug target

DRD2 is a well-established DA receptor, but how the diverse actions of DRD2s in multipartite, DA-sensitive circuits are coordinated to produce specific behaviors remains unclear (Gallo, 2019). The present study revealed the role of GPR143 in DRD2-mediated dopaminergic transmission. GPR143 is also expressed in a subset of DRD2-positive MSNs in the striatum. DRD2- or GPR143-positive, and this region contains both DRD2- and GPR143-positive MSNs (Masukawa et al., 2023). The expression pattern provides further evidence for the heterogeneity of DRD2-expressing neurons. Antipsychotics are used to relieve symptoms of neuropsychiatric disorders such as schizophrenia and mostly target DRD2 with a wide variety of pharmacologic properties. Our findings indicate that the L-DOPA-GPR143 signaling observed in cholinergic interneurons may be an underlying mechanism for the diversity of DRD2 functions, and will aid in improving therapeutic interventions for diseases associated with abnormal DA transmission.

References

Aosaki T, Tsubokawa H, Ishida A, Watanabe K, Graybiel AM, Kimura M (1994) Responses of tonically active neurons in the primate's striatum undergo systematic changes during behavioral sensorimotor conditioning. J Neurosci 14:3969–3984.

Bertran-Gonzalez J, Chieng BC, Laurent V, Valjent E, Balleine BW (2012) Striatal cholinergic interneurons display activity-related phosphorylation of ribosomal protein S6. PLoS One 7:e53195.

Cachope R, Mateo Y, Mathur BN, Irving J, Wang HL, Morales M, Lovinger DM, Cheer JF (2012) Selective activation of cholinergic interneurons enhances accumbal phasic dopamine release: setting the tone for reward processing. Cell Rep 2:33–41.

Crittenden JR, Graybiel AM (2011) Basal Ganglia disorders associated with imbalances in the striatal striosome and matrix compartments. Front Neuroanat 5:59.

DeBoer P, Heeringa MJ, Abercrombie ED (1996) Spontaneous release of acetylcholine in striatum is preferentially regulated by inhibitory dopamine D2 receptors. Eur J Pharmacol 317:257–262.

Dimova R, Vuillet J, Nieoullon A, Kerkerian-Le Goff L (1993) Ultrastructural features of the choline acetyltransferase-containing neurons and relationships with nigral dopaminergic and cortical afferent pathways in the rat striatum. Neuroscience 53:1059–1071.

Ding JB, Guzman JN, Peterson JD, Goldberg JA, Surmeier DJ (2010) Thalamic gating of corticostriatal signaling by cholinergic interneurons. Neuron 67:294–307.

Fukuda N, Naito S, Masukawa D, Kaneda M, Miyamoto H, Abe T, Yamashita Y, Endo I, Nakamura F, Goshima Y (2015) Expression of ocular albinism 1 (OA1), 3, 4-dihydroxy-L-phenylalanine (DOPA) receptor, in both neuronal and non-neuronal organs. Brain Res 1602:62–74.

Furukawa N, Goshima Y, Miyamae T, Sugiyama Y, Shimizu M, Ohshima E, Suzuki F, Arai N, Fujita K, Misu Y (2000) L-DOPA cyclohexyl ester is a novel potent and relatively stable competitive antagonist against L-DOPA among several L-DOPA ester compounds. Jpn J Pharmacol 82:40–47.

Gallo EF (2019) Disentangling the diverse roles of dopamine D2 receptors in striatal function and behavior. Neurochem Int 125:35–46.

Goshima Y, Masukawa D, Kasahara Y, Hashimoto T, Aladeokin AC (2019) l-DOPA and its receptor GPR143: implications for pathogenesis and therapy in Parkinson's disease. Front Pharmacol 10:1119.

Group PDMC, et al. (2014) Long-term effectiveness of dopamine agonists and monoamine oxidase B inhibitors compared with levodopa as initial treatment for Parkinson's disease (PD MED): a large, open-label, pragmatic randomised trial. Lancet 384:1196–1205.

Ikemoto K, Kitahama K, Nishimura A, Jouvet A, Nishi K, Arai R, Jouvet M, Nagatsu I (1999) Tyrosine hydroxylase and aromatic L-amino acid decarboxylase do not coexist in neurons in the human anterior cingulate cortex. Neurosci Lett 269:37–40.

Izawa J, Yamanashi K, Asakura T, Misu Y, Goshima Y (2006) Differential effects of methamphetamine and cocaine on behavior and extracellular levels of dopamine and 3,4-dihydroxyphenylalanine in the nucleus accumbens of conscious rats. Eur J Pharmacol 549:84–90.

Karasawa N, Isomura G, Nagatsu I (1992) Production of specific antibody against L-dopa and its ultrastructural localization of immunoreactivity in the house-shrew (Suncus murinus) lateral habenular nucleus. Neurosci Lett 143:267–270.

Kasahara Y, et al. (2021) Distribution of mRNA for GPR143, a receptor of 3,4-L-dihydroxyphenylalanine, and of immunoreactivities for nicotinic acetylcholine receptors in the nigrostriatal and mesolimbic regions. Neurosci Res 170:370–375.

Kasahara Y, Masukawa D, Kobayashi K, Yamasaki M, Watanabe M, Goshima Y (2022) L-DOPA-induced neurogenesis in the hippocampus is mediated through GPR143, a distinct mechanism of dopamine. Stem Cells 40:215–226.

Kharkwal G, Brami-Cherrier K, Lizardi-Ortiz JE, Nelson AB, Ramos M, Del Barrio D, Sulzer D, Kreitzer AC, Borrelli E (2016) Parkinsonism driven by antipsychotics originates from dopaminergic control of striatal cholinergic interneurons. Neuron 91:67–78.

Konno K, Yamasaki M, Miyazaki T, Watanabe M (2023) Glyoxal fixation: an approach to solve immunohistochemical problem in neuroscience research. Sci Adv 9:eadf7084.

Latif S, et al. (2021) Dopamine in Parkinson's disease. Clin Chim Acta 522: 114–126.

Lewis RG, Serra M, Radl D, Gori M, Tran C, Michalak SE, Vanderwal CD, Borrelli E (2020) Dopaminergic control of striatal cholinergic interneurons underlies cocaine-induced psychostimulation. Cell Rep 31: 107527.

Lopez VM, Decatur CL, Stamer WD, Lynch RM, McKay BS (2008) L-DOPA is an endogenous ligand for OA1. PLoS Biol 6:e236.

Masukawa D, et al. (2017) L-DOPA sensitizes vasomotor tone by modulating the vascular alpha1-adrenergic receptor. JCI Insight 2:e90903.

Masukawa D, et al. (2023) Coupling between GPR143 and dopamine D2 receptor is required for selective potentiation of dopamine D2 receptor function by L-3,4-dihydroxyphenylalanine in the dorsal striatum. J Neurochem 165:177–195.

Misu Y, Goshima Y, Ueda H, Okamura H (1996) Neurobiology of L-DOPAergic systems. Prog Neurobiol 49:415–454.

Nakamura S, Goshima Y, Yue JL, Miyamae T, Misu Y (1993) Endogenously released DOPA is probably relevant to nicotine-induced increases in locomotor activities of rats. Jpn J Pharmacol 62:107–110.

Nelson AB, Hammack N, Yang CF, Shah NM, Seal RP, Kreitzer AC (2014) Striatal cholinergic interneurons Drive GABA release from dopamine terminals. Neuron 82:63–70.

Pani L (2002) Clinical implications of dopamine research in schizophrenia. Curr Med Res Opin 18(Suppl 3):s3–s7.

Pickel VM, Chan J (1990) Spiny neurons lacking choline acetyltransferase immunoreactivity are major targets of cholinergic and catecholaminergic terminals in rat striatum. J Neurosci Res 25:263–280.

Schiaffino MV, et al. (1999) Ocular albinism: evidence for a defect in an intracellular signal transduction system. Nat Genet 23:108–112.

Straub C, Tritsch NX, Hagan NA, Gu C, Sabatini BL (2014) Multiphasic modulation of cholinergic interneurons by nigrostriatal afferents. J Neurosci 34:8557–8569.

Tepper JM, Bolam JP (2004) Functional diversity and specificity of neostriatal interneurons. Curr Opin Neurobiol 14:685–692.

Thorn CA, Graybiel AM (2010) Pausing to regroup: thalamic gating of cortico-basal ganglia networks. Neuron 67:175–178.

Threlfell S, Lalic T, Platt NJ, Jennings KA, Deisseroth K, Cragg SJ (2012) Striatal dopamine release is triggered by synchronized activity in cholinergic interneurons. Neuron 75:58–64.

Tison F, Mons N, Rouet-Karama S, Geffard M, Henry P (1989) Endogenous L-dopa in the rat dorsal vagal complex: an immunocytochemical study by light and electron microscopy. Brain Res 497:260–270.

Torigoe K, et al. (2012) Usefulness of olanzapine as an adjunct to opioid treatment and for the treatment of neuropathic pain. Anesthesiology 116:159–169.

Tozzi A, et al. (2011) The distinct role of medium spiny neurons and cholinergic interneurons in the D(2)/A(2)A receptor interaction in the striatum: implications for Parkinson's disease. J Neurosci 31:1850–1862.

Wada M, et al. (2022) Dopaminergic dysfunction and excitatory/inhibitory imbalance in treatment-resistant schizophrenia and novel neuromodulatory treatment. Mol Psychiatry 27:2950–2967.

Waku I, Magalhaes MS, Alves CO, de Oliveira AR (2021) Haloperidol-induced catalepsy as an animal model for parkinsonism: a systematic review of experimental studies. Eur J Neurosci 53:3743–3767.

Witten IB, Lin SC, Brodsky M, Prakash R, Diester I, Anikeeva P, Gradinaru V, Ramakrishnan C, Deisseroth K (2010) Cholinergic interneurons control local circuit activity and cocaine conditioning. Science 330:1677–1681.